Reaction Route Graphs. II. Examples of Enzyme- and Surface-Catalyzed Single Overall Reactions

Ilie Fishtik, Caitlin A. Callaghan, and Ravindra Datta*

Fuel Cell Center, Department of Chemical Engineering, Worcester Polytechnic Institute, Worcester, Massachusetts 01609

Received: November 7, 2003; In Final Form: February 11, 2004

The utility of the new reaction route (RR) graph theory developed in the preceding paper (Part I) is illustrated here, with the help of two examples. In the first example, the kinetics of the conversion of 7,8-dihydrofolate and NADPH to 5,6,7,8-tetrahydrofolate and NADP, as catalyzed by dihydrofolate reductase (DHFR), is considered. This system is described by a linear kinetic mechanism that includes 13 elementary reaction steps. The second example is a microkinetic model of the water-gas shift reaction on a copper catalyst, which is highly nonlinear and includes 15 elementary surface reaction steps. For both mechanisms, the RR graphs have been constructed and used to determine the overall rates. The RR graphs and the overall rate equations are further simplified and reduced, using the RR network approach.

1. Introduction

In a preceding paper, referenced here as Part I,[1] we have introduced a new type of graph, namely, a reaction route (RR) graph, G_R, for minimal, nonlinear, single overall reactions (OR) that are comprised of multiple RR kinetic mechanisms. This new type of graph has been shown to be ideally suited to depict reaction routes and mechanisms and to utilize the analogy between the reaction and electrical networks in a rigorous, quantitative manner. In particular, the old and intuitively appealing idea of visualizing the elementary reaction steps in a kinetic mechanism as resistors, the rates as currents, and the affinities as voltages can be utilized quantitatively via the natural translation of a RR graph into a RR network that fully resembles an electrical network. As a result, one can use the well-developed and powerful methods of electrical networks to rationalize, reduce, and simplify complex kinetic mechanisms.

Here, we illustrate the capabilities of the RR graph approach with the help of two examples, both of which have been widely investigated in the literature. The first involves an enzyme-catalyzed conversion of 7,8-dihydrofolate and NADPH into 5,6,7,8-tetrahydrofolate and NADP. It is a 13-elementary reaction step linear kinetic mechanism, i.e., the reaction steps are first-order, with respect to intermediates in either direction, and is, consequently, amenable to analysis via earlier graph-theoretic approaches. The second is a more-complex, nonlinear 15-elementary reaction step water-gas shift (WGS) reaction that is catalyzed by copper, which is not amenable to graph-theory analysis by existing approaches. The electrical analogy is utilized to simplify the kinetics and mechanism of the overall reactions for these two reactions.

2. Dihydrofolate Reductase (DHFR) System

The mechanism that describes the conversion of 7,8-dihydrofolate (A) and NADPH (B) to 5,6,7,8-tetrahydrofolate (C) and $NADP^+$ (D), as catalyzed by the enzyme dihydrofolate reductase (E), along with a set of rate constants is presented in Table 1.[2] This is a single OR of the type

$$A + B \leftrightarrows C + D$$

that involves multiple RRs. The kinetics of this reaction has been intensively investigated both experimentally[3−6] and theoretically, using the theory of direct RRs[2,7,8] and the conventional King−Altman formalism.[9−11] The enumeration of direct RRs in this system has been considered by Happel and Sellers.[2,7,8] Their results are presented in Table 2. Of course, alternately, these RRs may be enumerated, as per the algorithm that was described in Part I.[1]

The rate constants of the elementary reaction steps used in previous publications[2−9] are not thermodynamically consistent; i.e., Kirchhoff's Voltage Law (KVL) is not followed, because it is rendered transparent by the current approach. In other words, the affinity of the overall reaction expressed via the affinities of the elementary reaction steps takes on slightly different values for different RRs. Alternatively, the affinities of the elementary reaction steps that comprise empty routes

TABLE 1: Elementary Reaction Steps and Their Rates in the Dihydrofolate Reductase (DHFR) System[a]

step	reaction	simplified rate
s_1	E + B = EB	$r_1 = 38.0[E][B] - 1.7[EB]$
s_2	EB + A = EAB	$r_2 = 100.2[A][EB] - 94.0[EAB]$
s_3	E + A = EA	$r_3 = 264.0[A][E] - 14.0[EA]$
s_4	EA+ B = EAB	$r_4 = 24.0[B][EA] - 19.0[EAB]$
s_5	EAB = ECD	$r_5 = 1360.0[EAB] - 37.0[ECD]$
s_6	EC = E + C	$r_6 = 5.1[EC] - 117.0[C][E]$
s_7	ECD = D + EC	$r_7 = 57.9[ECD] - 0.7[D][EC]$
s_8	ECD = C + ED	$r_8 = 46.0[ECD] - 24.0[C][ED]$
s_9	ED = D + E	$r_9 = 32.0[ED] - 17.0[D][E]$
s_{10}	EB + C = EBC	$r_{10} = 14.0[C][EB] - 225.0[EBC]$
s_{11}	EC + B = EBC	$r_{11} = 4.4[B][EC] - 72.6[EBC]$
s_{12}	EA + D = EAD	$r_{12} = 11.0[D][EA] - 4.6[EAD]$
s_{13}	ED + A = EAD	$r_{13} = 110.0[A][ED] - 1.3[EAD]$

[a] From ref 2.

* Author to whom correspondence should be addressed. E-mail address: rdatta@wpi.edu.

10.1021/jp037401w CCC: $27.50
Published on Web 04/07/2004

TABLE 2. Stoichiometrically Distinct RRs for the DFHS System[a]

reaction route	expression
	Full RRs
RR_1	$OR = s_3 + s_4 + s_5 + s_8 + s_9$
RR_2	$OR = s_3 + s_4 + s_5 + s_6 + s_7$
RR_3	$OR = s_2 + s_5 + s_7 - s_{10} + s_{11}$
RR_4	$OR = s_2 + s_5 - s_6 + s_8 + s_9 - s_{10} + s_{11}$
RR_5	$OR = s_1 + s_2 + s_5 + s_8 + s_9$
RR_6	$OR = s_1 + s_2 + s_5 + s_6 + s_7$
RR_7	$OR = -s_1 + s_3 + s_4 + s_5 + s_7 - s_{10} + s_{11}$
RR_8	$OR = s_4 + s_5 + s_8 - s_{12} + s_{13}$
RR_9	$OR = s_4 + s_5 + s_6 + s_7 - s_9 - s_{12} + s_{13}$
RR_{10}	$OR = -s_1 + s_4 + s_5 + s_7 - s_9 - s_{10} + s_{11} - s_{12} + s_{13}$
RR_{11}	$OR = s_2 - s_3 + s_5 - s_6 + s_8 - s_{10} + s_{11} - s_{12} + s_{13}$
RR_{12}	$OR = s_1 + s_2 - s_3 + s_5 + s_8 - s_{12} + s_{13}$
	Empty RRs
ER_1	$s_1 + s_2 - s_3 - s_4 = 0$
ER_2	$s_1 + s_6 + s_{10} - s_{11} = 0$
ER_3	$s_1 - s_7 + s_8 + s_9 + s_{10} - s_{11} = 0$
ER_4	$s_2 - s_3 - s_4 - s_6 - s_{10} + s_{11} = 0$
ER_5	$s_2 - s_3 - s_4 + s_7 - s_8 - s_9 - s_{10} + s_{11} = 0$
ER_6	$s_6 + s_7 - s_8 - s_9 = 0$
ER_7	$s_3 + s_9 + s_{12} - s_{13} = 0$
ER_8	$-s_2 + s_4 + s_6 - s_9 + s_{10} - s_{11} - s_{12} + s_{13} = 0$
ER_9	$-s_3 - s_6 - s_7 + s_8 - s_{12} + s_{13} = 0$
ER_{10}	$-s_2 + s_4 - s_7 + s_8 + s_{10} - s_{11} - s_{12} + s_{13} = 0$
ER_{11}	$s_1 - s_3 - s_7 + s_8 + s_{10} - s_{11} - s_{12} + s_{13} = 0$

[a] From ref 2.

(ERs) do not sum to zero. For instance, from Table 2, for ER_2, i.e.,

$$s_1 + s_6 + s_{10} - s_{11} = 0$$

the affinities follow

$$A_1 + A_6 + A_{10} - A_{11} = 0$$

In turn, according to eq 28 from Part I,[1] the rate constants of these elementary reaction steps are subject to the following constraint:

$$\left(\frac{\vec{k}_1}{\overleftarrow{k}_1}\right)\left(\frac{\vec{k}_6}{\overleftarrow{k}_6}\right)\left(\frac{\vec{k}_{10}}{\overleftarrow{k}_{10}}\right)\left(\frac{\vec{k}_{11}}{\overleftarrow{k}_{11}}\right)^{-1} = 1$$

Using the data from ref 2, it can be readily verified that this product is equal to 1.378 rather than 1. To eliminate this thermodynamic inconsistency, we have modified the rate constant in the reverse direction for reaction s_{11}; i.e., the original value $\vec{k}_{11} = 100$ has been replaced with $\vec{k}_{11} = 72.57$. Other reaction constants that have been modified include $\vec{k}_2$, $\vec{k}_7$, and $\vec{k}_{12}$. Note that these modifications do not affect the overall kinetics of the process.

For the purpose of this illustration, all of the numerical simulations described below for this system were performed for a batch reactor under the following set of initial conditions:[7,8,10] [A] = [B] = 0.9, [C] = [D] = 0.1, and [E] = 1, whereas [EA] = [EB] = [AC] = [ES] = [EAB] = [EBC] = [ECD] = [EAD] = 0, in arbitrary units. The numerical results were used to compute reaction-step resistances and affinities as described in Part I.[1]

2.1. Construction of the RR Graph. The system is comprised of $q = 8$ independent intermediates (EA, EB, EC, ED, EAB, ECD, EBC, and EAD) and $n = 4$ terminal species (A, B, C, and D). Our starting point in the construction of the RR graph is the overall stoichiometric matrix

$\boldsymbol{\nu} =$

EA	EB	EC	ED	EAB	EBC	ECD	EAD	A	B	C	D	
0	0	0	0	0	0	0	0	−1	−1	+1	+1	OR
0	+1	0	0	0	0	0	0	0	−1	0	0	s_1
0	−1	0	0	+1	0	0	0	−1	0	0	0	s_2
+1	0	0	0	0	0	0	0	−1	0	0	0	s_3
−1	0	0	0	+1	0	0	0	0	−1	0	0	s_4
0	0	0	0	−1	0	+1	0	0	0	0	0	s_5
0	0	−1	0	0	0	0	0	0	0	+1	0	s_6
0	0	+1	0	0	0	−1	0	0	0	0	+1	s_7
0	0	0	+1	0	0	−1	0	0	0	+1	0	s_8
0	0	0	−1	0	0	0	0	0	0	0	+1	s_9
0	−1	0	0	0	+1	0	0	0	0	−1	0	s_{10}
0	0	−1	0	0	+1	0	0	0	−1	0	0	s_{11}
−1	0	0	0	0	0	0	+1	0	0	0	−1	s_{12}
0	0	0	−1	0	0	0	+1	−1	0	0	0	s_{13}

Because the concentrations of the intermediates are subject to an enzyme balance, E is eliminated from the aforementioned consideration:

$$[E] + [EA] + [EB] + [EC] + [ED] + [EAB] + [ECD] + [EBC] + [EAD] = [E_0]$$

where $[E_0]$ is the total concentration of enzyme. Therefore, because $q = \text{rank } \boldsymbol{\alpha} = 8$, the number of nodes in the RR graph is equal to $N = q + 2 = 8 + 2 = 10$. As shown in Part I,[1] the incidence matrix $\mathbf{M}$ of the RR graph may be obtained by performing row operations on the transposed overall stoichiometric matrix $\boldsymbol{\nu}^T$. After a series of elementary row operations such that each column has no more than one +1 value and one −1 value, with the balance of elements being zero, we obtain

$\mathbf{M} =$

OR	s_1	s_2	s_3	s_4	s_5	s_6	s_7	s_8	s_9	s_{10}	s_{11}	s_{12}	s_{13}	
+1	0	+1	0	+1	0	0	0	0	0	0	0	0	0	n_1
0	+1	−1	0	0	0	0	0	0	0	−1	0	0	0	n_2
0	0	0	+1	−1	0	0	0	0	0	0	0	−1	0	n_3
0	−1	0	−1	0	0	+1	0	0	+1	0	0	0	0	n_4
0	0	0	0	0	0	0	0	0	0	+1	+1	0	0	n_5
0	0	0	0	0	0	0	0	0	0	0	0	+1	+1	n_6
0	0	0	0	0	0	−1	+1	0	0	0	−1	0	0	n_7
0	0	0	0	0	0	0	0	+1	−1	0	0	0	−1	n_8
0	0	0	0	0	+1	0	−1	−1	0	0	0	0	0	n_9
−1	0	0	0	0	−1	0	0	0	0	0	0	0	0	n_{10}

The RR graph corresponding to this kinetic mechanism is easily drawn and is shown in Figure 1. It is evident that the reaction graph incorporates the complete list of both full and empty RRs listed in Table 2. For comparison, we present, in Figure 2, the conventional reaction graph[10] (i.e., a graph in which the nodes represent the intermediates, because it is possible to do so in this linear kinetic mechanism). It can be seen that the conventional graph is not amenable to RR analysis. Thus, to get a complete set of direct RRs, one must use three different starting and ending points on the graph.

Alternatively, as described in Part I,[1] the RR graph may be constructed from an arbitrarily selected set of linearly independent RRs, chosen from Table 2. According to the Horiuti−Temkin theorem,[12] the number of linearly independent RRs for this system is equal to $L = p - \text{rank } \boldsymbol{\alpha} = 13 - 8 = 5$. These five independent RRs may be arbitrarily selected from the list

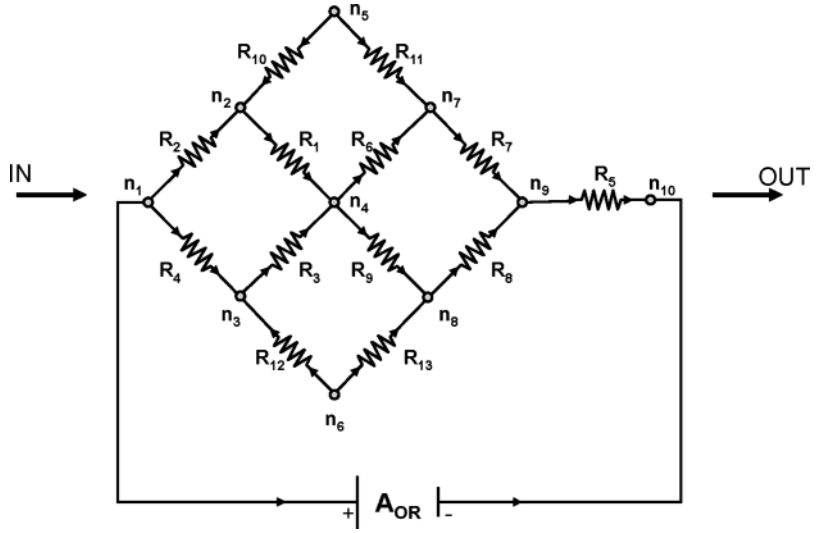

Figure 1. Reaction route (RR) graph for the dihydrofolate reductase (DHFR) system.

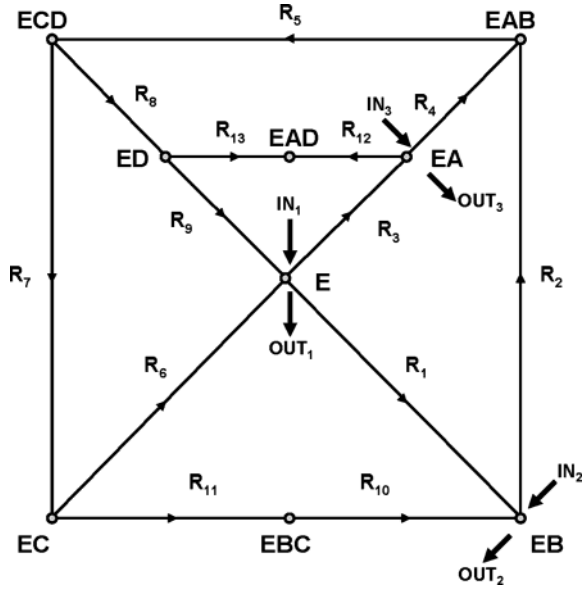

Figure 2. Conventional kinetic graph for the DHFR system (adapted from ref 10).

of direct RRs in Table 2. For example, one set of five linearly independent RRs is

$$\mathrm{RR_I} = s_1 + s_2 - s_3 - s_4 = \mathrm{ER_1}$$

$$\mathrm{RR_{II}} = s_3 + s_4 + s_5 + s_6 + s_7 = \mathrm{RR_2}$$

$$\mathrm{RR_{III}} = s_3 + s_4 + s_5 + s_8 + s_9 = \mathrm{RR_1}$$

$$\mathrm{RR_{IV}} = -s_1 + s_3 + s_4 + s_5 + s_7 - s_{10} + s_{11} = \mathrm{RR_7}$$

$$\mathrm{RR_V} = s_4 + s_5 + s_8 - s_{12} + s_{13} = \mathrm{RR_8}$$

As can be seen, the first RR from this set is an empty RR. Indeed,

s_1:	$\mathrm{E + B \leftrightarrows EB}$	$(\sigma_j = 1)$
s_2:	$\mathrm{EB + A \leftrightarrows EAB}$	$(\sigma_j = 1)$
s_3:	$\mathrm{E + A \leftrightarrows EA}$	$(\sigma_j = -1)$
s_4:	$\mathrm{EA + B \leftrightarrows EAB}$	$(\sigma_j = -1)$
Net:	$0 \leftrightarrows 0$	

However, the next four RRs are full. For instance, the second RR is

s_3:	$\mathrm{E + A \leftrightarrows EA}$	$(\sigma_j = 1)$
s_4:	$\mathrm{EA + B \leftrightarrows EAB}$	$(\sigma_j = 1)$
s_5:	$\mathrm{EAB \leftrightarrows ECD}$	$(\sigma_j = 1)$
s_6:	$\mathrm{EC \leftrightarrows E + C}$	$(\sigma_j = 1)$
s_7:	$\mathrm{ECD \leftrightarrows D + EC}$	$(\sigma_j = 1)$
Net:	$\mathrm{A + B \leftrightarrows C + D}$	

After the elementary reaction steps are reordered, the fundamental RR matrix may be presented in the form

$\boldsymbol{\sigma}_\mathrm{f} =$

	twigs								links				
OR	s_1	s_2	s_3	s_4	s_5	s_6	s_7	s_8	s_9	s_{10}	s_{11}	s_{12}	s_{13}	
0	+1	−1	−1	0	0	0	0	0	+1	0	0	0	0	$\mathrm{RR_I}$
−1	0	+1	+1	+1	+1	0	0	0	0	+1	0	0	0	$\mathrm{RR_{II}}$
−1	0	+1	+1	+1	0	+1	0	0	0	0	+1	0	0	$\mathrm{RR_{III}}$
−1	−1	+1	+1	+1	+1	0	−1	0	0	0	0	+1	0	$\mathrm{RR_{IV}}$
−1	0	0	+1	+1	0	+1	0	−1	0	0	0	0	+1	$\mathrm{RR_V}$

Using eq 19 from Part I[1] results in the following fundamental cut-set matrix:

$\mathbf{X}_\mathrm{f} =$

	twigs								links				
OR	s_1	s_2	s_3	s_4	s_5	s_6	s_7	s_8	s_9	s_{10}	s_{11}	s_{12}	s_{13}
+1	0	0	0	0	0	0	0	0	0	+1	+1	+1	+1
0	+1	0	0	0	0	0	0	0	−1	0	0	+1	0
0	0	+1	0	0	0	0	0	0	+1	−1	−1	−1	0
0	0	0	+1	0	0	0	0	0	+1	−1	−1	−1	−1
0	0	0	0	+1	0	0	0	0	0	−1	−1	−1	−1
0	0	0	0	0	+1	0	0	0	0	−1	0	−1	0
0	0	0	0	0	0	+1	0	0	0	0	−1	0	−1
0	0	0	0	0	0	0	+1	0	0	0	0	+1	0
0	0	0	0	0	0	0	0	+1	0	0	0	0	+1

The incidence matrix **M** may next be readily obtained by

elementary row operations on $\mathbf{X}_f$, followed by the addition of one more row, as described in Part I.[1]

2.2. Application of Kirchhoff's Laws. Based on the RR graph and the use of the electrical analogy, the overall rate r_{OR} is simply equal to the ratio between the affinity of the overall reaction A_{OR} and the overall resistance R_{OR} of the network:

$$r_{OR} = \frac{A_{OR}}{R_{OR}} \tag{1}$$

Recall that KVL and KCL may be written as $\mathbf{A}^{(l)} = -\boldsymbol{\sigma}_t \mathbf{A}^{(t)}$ and $\boldsymbol{r}^{(t)} = \boldsymbol{\sigma}_t^T \boldsymbol{J}$, respectively. By the convention adopted in Part I, $r_0 = -r_{OR}$, along with $\boldsymbol{r}^{(l)} = \boldsymbol{J}$, the following relationships for the link affinities, in terms of the twig affinities, and the twig rates, in terms of the link rates, are derived. For KVL:

$$A_1 + A_2 - A_3 - A_4 = 0$$
$$A_{OR} = A_3 + A_4 + A_5 + A_6 + A_{10}$$
$$A_{OR} = A_3 + A_4 + A_5 + A_8 + A_9$$
$$A_{OR} = A_1 + A_3 + A_4 + A_5 - A_{10} + A_{11}$$
$$A_{OR} = A_4 + A_5 + A_8 - A_{12} + A_{13}$$

KCL has two sets of rate expressions. One data set applies to $\boldsymbol{r}^{(t)} = \boldsymbol{\sigma}_t^T \boldsymbol{J}$:

$$r_{OR} = J_{II} + J_{III} + J_{IV} + J_V$$
$$r_1 = J_I - J_{IV}$$
$$r_3 = -J_I + J_{II} + J_{III} + J_{IV}$$
$$r_4 = -J_I + J_{II} + J_{III} + J_{IV}$$
$$r_5 = J_{II} + J_{III} + J_{IV} + J_V$$
$$r_7 = J_{II} + J_{IV}$$
$$r_8 = J_{III} + J_V$$
$$r_{10} = -J_{IV}$$
$$r_{12} = -J_V$$

The other data set applies to $\boldsymbol{r}^{(l)} = \boldsymbol{J}$:

$$r_2 = J_I$$
$$r_6 = J_{II}$$
$$r_9 = J_{III}$$
$$r_{11} = J_{IV}$$
$$r_{13} = J_V$$

Note that the first KVL equation is representative of an empty RR, and hence, the sum of the affinities involved is equal to zero.

In turn, the overall resistance may be evaluated from the individual resistances of the elementary reaction steps, using the conventional electrical circuit theory.[1] The procedure, which involves a series of $\Delta-Y$ conversions, is illustrated in Figure 3 and is comprised of the following steps. First, we add the resistances that are connected in series (i.e., $R_{10} + R_{11}$, $R_{12} + R_{13}$) and rearrange the graph as shown in Figure 3a. Second, we apply a set of $\Delta-Y$ conversions, thus arriving at Figure 3b. Third, after again combining the resistances in series, a second set of $\Delta-Y$ conversions is applied and the graph is rearranged according to Figure 3c. A final set of $\Delta-Y$ conversions results in a simple network (Figure 3d) that yields the following expression for the overall resistance:

$$R_{OR} = R_D + R_G + R_5 + \left(\frac{1}{R_E + R_{E'}} + \frac{1}{R_F + R_{F'}}\right) \tag{2}$$

where

$$R_A = \frac{R_1(R_{10} + R_{11})}{R_1 + R_6 + (R_{10} + R_{11})}$$
$$R_{A'} = \frac{R_3(R_{12} + R_{13})}{R_3 + R_9 + (R_{12} + R_{13})}$$
$$R_B = \frac{R_6(R_{10} + R_{11})}{R_1 + R_6 + (R_{10} + R_{11})}$$
$$R_{B'} = \frac{R_9(R_{12} + R_{13})}{R_3 + R_9 + (R_{12} + R_{13})}$$
$$R_C = \frac{R_1 R_6}{R_1 + R_6 + (R_{10} + R_{11})}$$
$$R_{C'} = \frac{R_3 R_9}{R_3 + R_9 + (R_{12} + R_{13})}$$
$$R_D = \frac{(R_2 + R_A)(R_4 + R_{A'})}{(R_2 + R_A) + (R_4 + R_{A'}) + (R_C + R_{C'})}$$
$$R_E = \frac{(R_2 + R_A)(R_C + R_{C'})}{(R_2 + R_A) + (R_4 + R_{A'}) + (R_C + R_{C'})}$$
$$R_{E'} = \frac{(R_7 + R_B)(R_C + R_{C'})}{(R_7 + R_B) + (R_8 + R_{B'}) + (R_C + R_{C'})}$$
$$R_F = \frac{(R_4 + R_{A'})(R_C + R_{C'})}{(R_2 + R_A) + (R_4 + R_{A'}) + (R_C + R_{C'})}$$
$$R_{F'} = \frac{(R_8 + R_{B'})(R_C + R_{C'})}{(R_7 + R_B) + (R_8 + R_{B'}) + (R_C + R_{C'})}$$
$$R_G = \frac{(R_7 + R_B)(R_8 + R_{B'})}{(R_7 + R_B) + (R_8 + R_{B'}) + (R_C + R_{C'})}$$

The overall rate, as a function of time in a batch reactor for the conditions previously mentioned, is presented in Figure 4.

2.3. Simplification and Reduction of the RR Network. Next, we analyze the RR graph with a focus on simplification and reduction. This can be achieved by evaluating the resistances along parallel pathways between two nodes separately. In Figures 5 and 6, we compare the pathways between nodes n_2 and n_7 and nodes n_3 and n_8, respectively. It is seen that there are sufficient differences in the resistances to justify neglecting the pathways that consist of $R_{10} + R_{11}$ and $R_{12} + R_{13}$ (see Figure 3a). Concomitantly, neglecting these pathways does not affect the overall resistance of the RR network. Figures 7 and 8 provide a similar comparison between the pathways that involve nodes n_1 and n_4 and nodes n_4 and n_9. Here, however, the resistances are sufficiently similar that no further reduction may be performed. We thus conclude that the elementary reaction steps

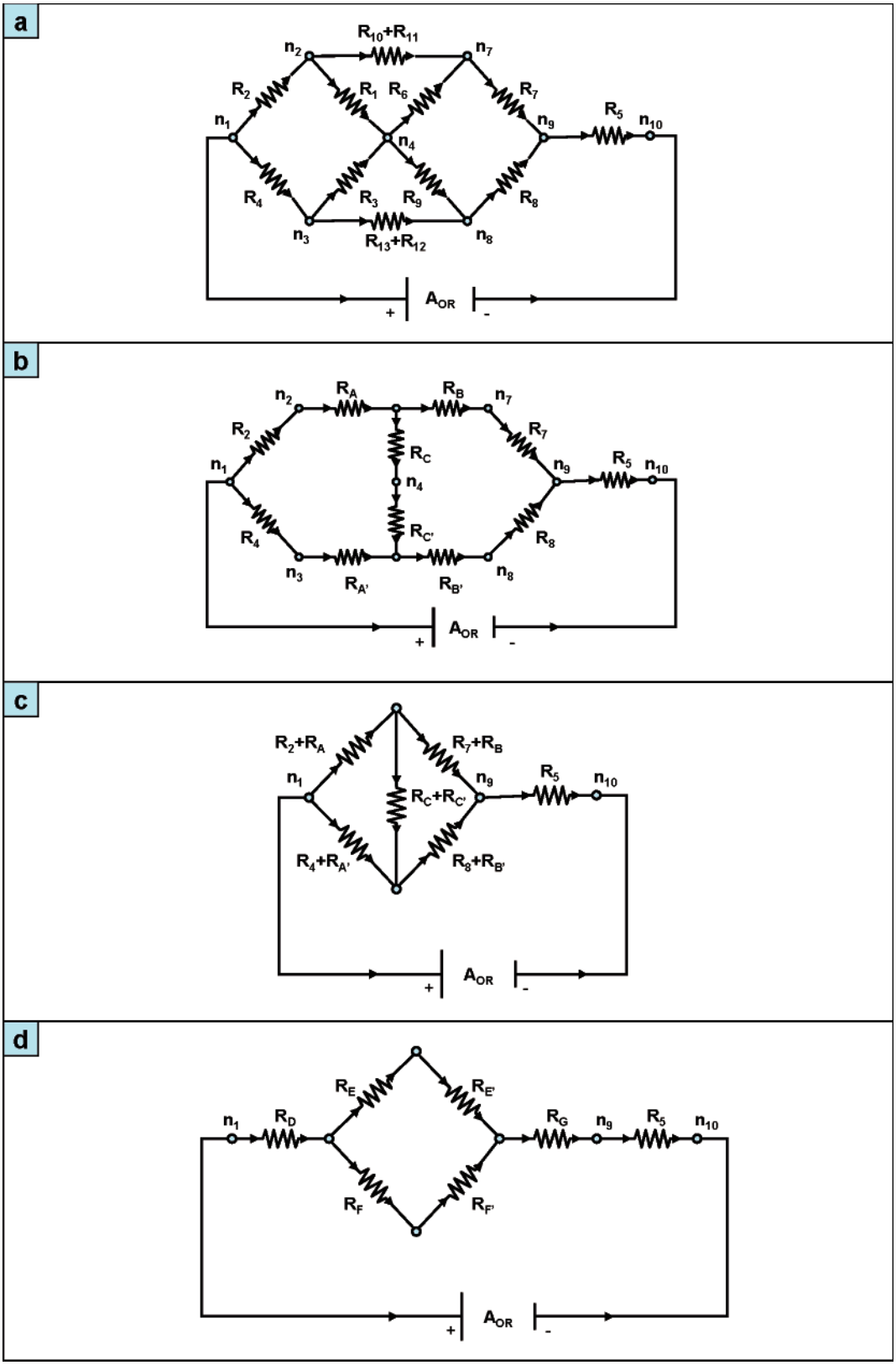

Figure 3. Evaluation of the overall resistance for the DHFR system.

s_{10}, s_{11}, s_{12}, and s_{13} may be dropped from the mechanism. As a result, the overall resistance of the reaction network is substantially simplified:

$$R_{OR} = \left(\frac{1}{R_1 + R_2} + \frac{1}{R_3 + R_4}\right)^{-1} + \left(\frac{1}{R_6 + R_7} + \frac{1}{R_8 + R_9}\right)^{-1} + R_5 \quad (3)$$

As shown in Figure 4, the simplified overall rate is in good agreement with the overall rate of the complete network.

3. Water-Gas Shift Reaction on Copper

Because of its industrial significance, the catalysis and kinetics of the water-gas shift (WGS) reaction has been one of the most extensively studied examples in microkinetic modeling.[13−21]

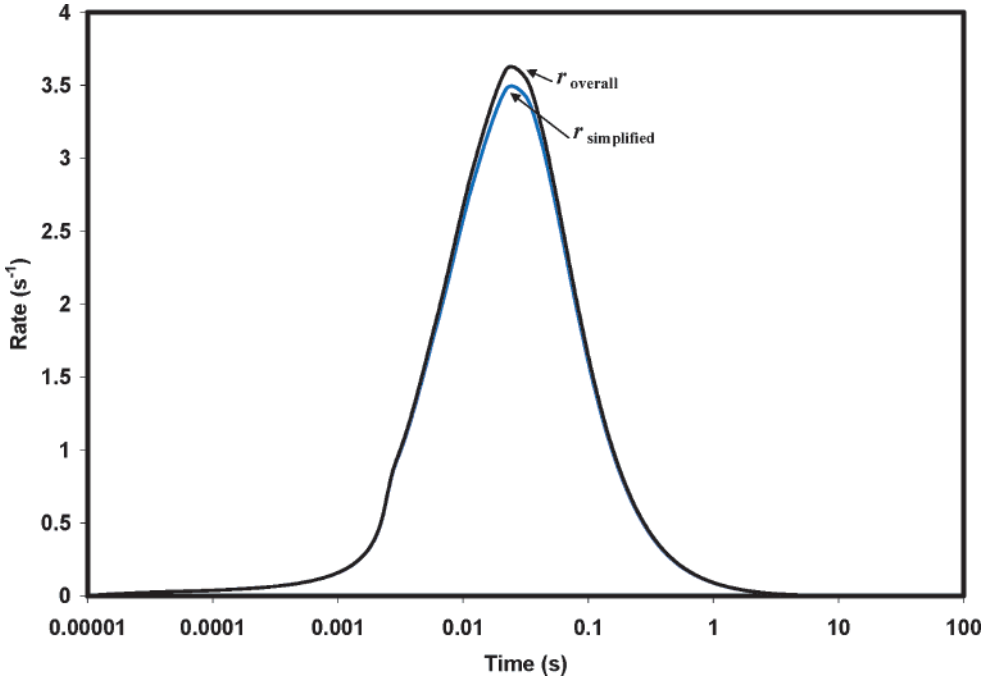

Figure 4. Overall rate versus the simplified rate, as a function of time for the DHFR reaction.

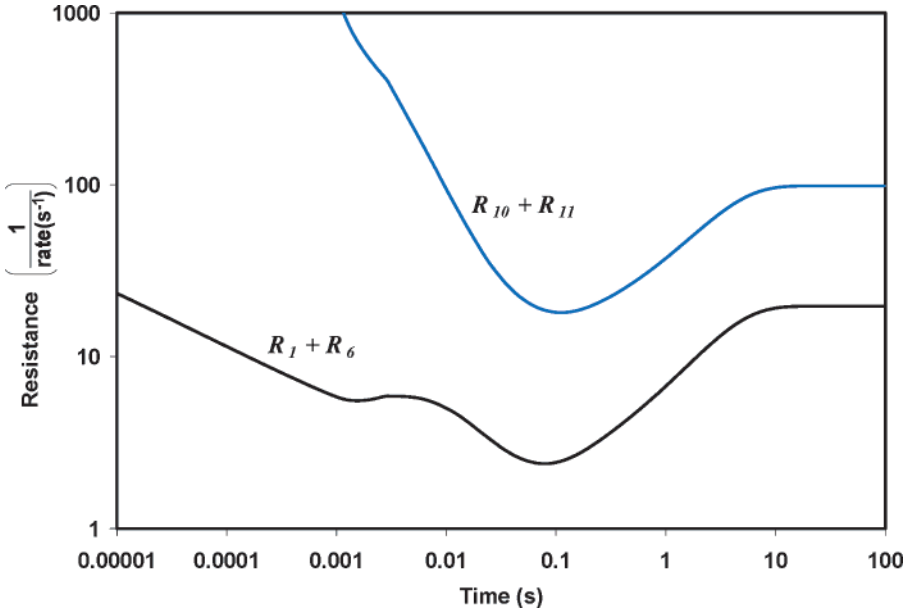

Figure 5. $R_{10} + R_{11}$ vs $R_1 + R_6$, as a function of time for the DHFR reaction in a batch reactor.

Even though it is not yet possible to make accurate ab initio predictions of rate constants on a given catalyst, we have recently shown[22,23] that a reliable predictive microkinetic model for the WGS reaction on copper may be developed based on the energetic characteristics of the elementary reaction steps calculated using the Unity Bond Index−Quadratic Exponential Potential (UBI−QEP) method developed by Shustorovich,[24] whereas the pre-exponential factors are estimated from the basic transition-state theory.[21,25] Here, to illustrate the RR graph approach developed in Part I,[1] we use a simplified, 15-elementary reaction step version of the complete 17-elementary reaction step microkinetic WGS reaction model (Table 3) that we developed earlier.[23,26] More specifically, we disregard two elementary reaction steps—namely, s_{13} and s_{16}—from the complete kinetic model for two reasons. First, it has been shown that the contributions to the overall mechanism and kinetics coming from these elementary reaction steps are negligibly small.[23] More significantly, however, neglecting s_{13} and s_{16} makes the stoichiometric numbers σ_{kh} in the resulting RRs equal to +1 or −1, thus allowing the use of the theory developed in Part I[1] for minimal mechanisms and RR graphs. The generalization of the theory to allow the inclusion of such steps will be subsequently addressed. However, note that the simplified, $p = 15$ (15 elementary reaction steps) version of the microkinetic mechanism of the WGS reaction on copper presented in Table 3 is highly nonlinear in that many reactions involve nonunit orders of the intermediates. The following numerical simulations were performed for a well-mixed flow reactor under the same conditions as those described in ref 22. These results were used to compute reaction affinities and resistances as described in Part I of this series.[1]

3.1. Construction of the RR Graph. The microkinetic model previously described is comprised of nine surface intermediates (H_2OS, COS, CO_2S, H_2S, HS, OHS, OS, HCOOS, S) and four

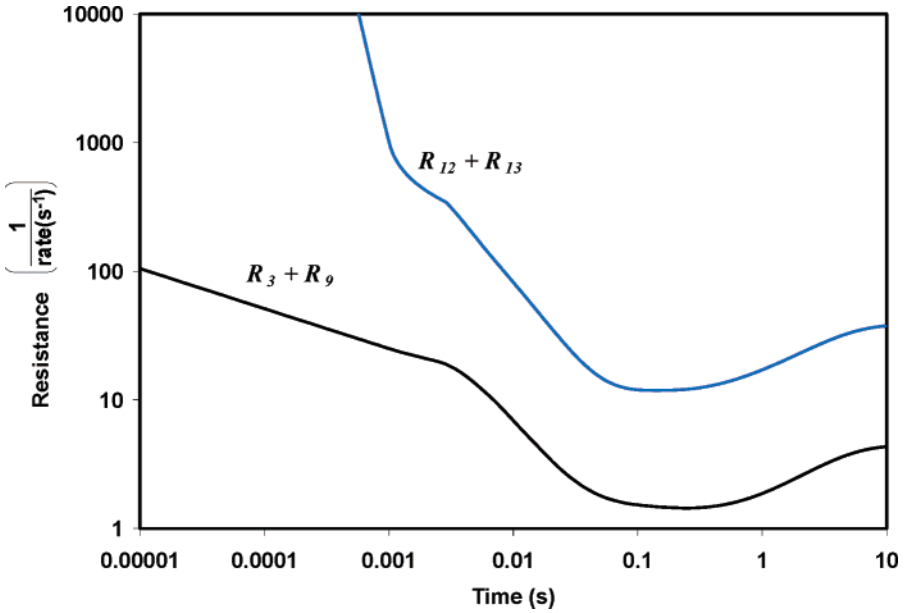

Figure 6. $R_{12} + R_{13}$ vs $R_3 + R_9$, as a function of time for the DHFR reaction in a batch reactor.

terminal species (H_2O, CO, CO_2, H_2). By virtue of the site balance, only $q = 8$ of the intermediates are linearly independent. Hence, S is neglected, as mentioned in Part I.[1] Thus, there are $N = q + 2 = 10$ nodes and $B = p + \mathrm{OR} = 16$ branches.

The overall stoichiometric matrix is

$\boldsymbol{\nu} =$

H_2OS	COS	CO_2S	H_2S	HS	OHS	OS	HCOOS	H_2O	CO	CO_2	H_2	
0	0	0	0	0	0	0	0	−1	−1	+1	+1	OR
0	+1	0	0	0	0	0	0	0	−1	0	0	s_1
+1	0	0	0	0	0	0	0	−1	0	0	0	s_2
0	0	−1	0	0	0	0	0	0	0	+1	0	s_3
0	0	0	+1	−2	0	0	0	0	0	0	0	s_4
0	0	0	−1	0	0	0	0	0	0	0	+1	s_5
−1	0	0	+1	0	+1	0	0	0	0	0	0	s_6
0	−1	−1	0	0	0	−1	0	0	0	0	0	s_7
0	0	0	+1	0	−1	+1	0	0	0	0	0	s_8
0	−1	+1	+1	0	−1	0	0	0	0	0	0	s_9
0	−1	+1	0	+1	−1	0	0	0	0	0	0	s_{10}
0	0	+1	0	+1	0	0	−1	0	0	0	0	s_{11}
0	0	+1	0	0	+1	−1	−1	0	0	0	0	s_{12}
−1	0	0	−1	−1	+1	0	0	0	0	0	0	s_{14}
0	0	0	+1	−1	−1	+1	0	0	0	0	0	s_{15}
0	0	+1	+1	−1	0	0	−1	0	0	0	0	s_{17}

The incidence matrix **M** of the RR graph is derived next, by performing elementary row operations on $\boldsymbol{\nu}^T$, as described in Part I:[1]

M =

OR	s_1	s_2	s_3	s_4	s_5	s_6	s_7	s_8	s_9	s_{10}	s_{11}	s_{12}	s_{14}	s_{15}	s_{17}	
+1	+1	0	0	0	0	0	0	0	0	0	0	0	0	0	0	n_1
0	−1	+1	0	0	0	0	0	0	0	0	0	0	0	0	0	n_2
0	0	−1	0	0	0	+1	0	0	0	0	0	0	+1	0	0	n_3
0	0	0	0	+1	0	−1	0	0	0	0	0	0	0	+1	+1	n_4
0	0	0	0	−1	0	0	0	0	+1	+1	+1	0	−1	0	0	n_5
0	0	0	0	0	0	0	0	+1	0	0	−1	−1	0	0	−1	n_6
0	0	0	0	0	0	0	+1	0	−1	0	0	+1	0	−1	0	n_7
0	0	0	+1	0	0	0	−1	−1	0	−1	0	0	0	0	0	n_8
0	0	0	−1	0	+1	0	0	0	0	0	0	0	0	0	0	n_9
−1	0	0	0	0	−1	0	0	0	0	0	0	0	0	0	0	n_{10}

The resulting RR graph is shown in Figure 9. An inspection reveals that the RR network involves all the full and empty RRs enumerated using the conventional algorithm (Table 4).[23] However, the RR graph is far more revealing, in terms of the reaction interconnections and the different pathways taken by reactants to form products.

3.2. Linearly Independent RRs and Kirchhoff's Laws. For the kinetic analysis of the WGS reaction mechanism, we must further select a set of linearly independent RRs. The total number of linearly independent RRs, as per the Horiuti−Temkin theorem, is $L = p - q = 15 - 8 = 7$. Let us arbitrarily choose the following set of linearly independent RRs from the list of direct RRs in Table 4 for the purpose of illustration:

$$\mathrm{RR_I} = s_1 + s_2 + s_3 + s_4 + s_5 + s_6 + s_7 + 0s_8 + s_9$$

$$\mathrm{RR_{II}} = s_1 + s_2 + s_3 + s_4 + s_5 + s_6 + 0s_7 + 0s_8 + s_{10}$$

$$\mathrm{RR_{III}} = s_1 + s_2 + s_3 + s_4 + s_5 + s_6 + 0s_7 + s_8 + s_{11}$$

$$\mathrm{RR_{IV}} = 0s_1 + 0s_2 + 0s_3 + 0s_4 + 0s_5 + 0s_6 - s_7 + s_8 + s_{12}$$

$$\mathrm{RR_V} = 0s_1 + 0s_2 + 0s_3 - s_4 + 0s_5 - s_6 + 0s_7 + 0s_8 + s_{14}$$

$$\mathrm{RR_{VI}} = s_1 + s_2 + s_3 + 0s_4 + s_5 + s_6 + s_7 + 0s_8 + s_{15}$$

$$\mathrm{RR_{VII}} = s_1 + s_2 + s_3 + 0s_4 + s_5 + s_6 + 0s_7 + s_8 + s_{17}$$

where it may be noticed, from Table 4, that $\mathrm{RR_I} = \mathrm{RR_1}$, $\mathrm{RR_{II}} = \mathrm{RR_2}$, $\mathrm{RR_{III}} = \mathrm{RR_3}$, $\mathrm{RR_{IV}} = \mathrm{ER_{25}}$, $\mathrm{RR_V} = \mathrm{ER_4}$, $\mathrm{RR_{VI}} = \mathrm{RR_6}$, and $\mathrm{RR_{VII}} = \mathrm{RR_{17}}$. One may, of course, select an alternate independent set. The chosen set provides the following independent fundamental RR matrix:

$\boldsymbol{\sigma}_f =$

	twigs								links							
OR	s_1	s_2	s_3	s_4	s_5	s_6	s_7	s_8	s_9	s_{10}	s_{11}	s_{12}	s_{14}	s_{15}	s_{17}	
−1	+1	+1	+1	+1	+1	+1	+1	0	+1	0	0	0	0	0	0	$\mathrm{RR_I}$
−1	+1	+1	+1	+1	+1	+1	0	0	0	+1	0	0	0	0	0	$\mathrm{RR_{II}}$
−1	+1	+1	+1	+1	+1	+1	0	+1	0	0	+1	0	0	0	0	$\mathrm{RR_{III}}$
0	0	0	0	0	0	0	−1	+1	0	0	0	+1	0	0	0	$\mathrm{RR_{IV}}$
0	0	0	0	−1	0	−1	0	0	0	0	0	0	+1	0	0	$\mathrm{RR_V}$
−1	+1	+1	+1	0	+1	+1	+1	0	0	0	0	0	0	+1	0	$\mathrm{RR_{VI}}$
−1	+1	+1	+1	0	+1	+1	0	+1	0	0	0	0	0	0	+1	$\mathrm{RR_{VII}}$

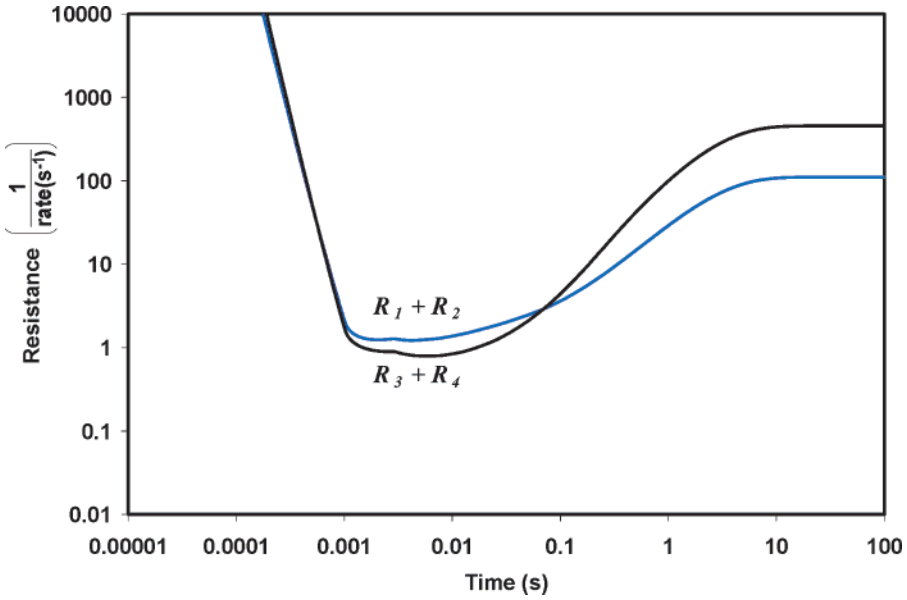

Figure 7. $R_1 + R_2$ vs $R_3 + R_4$, as a function of time for the DHFR reaction in a batch reactor.

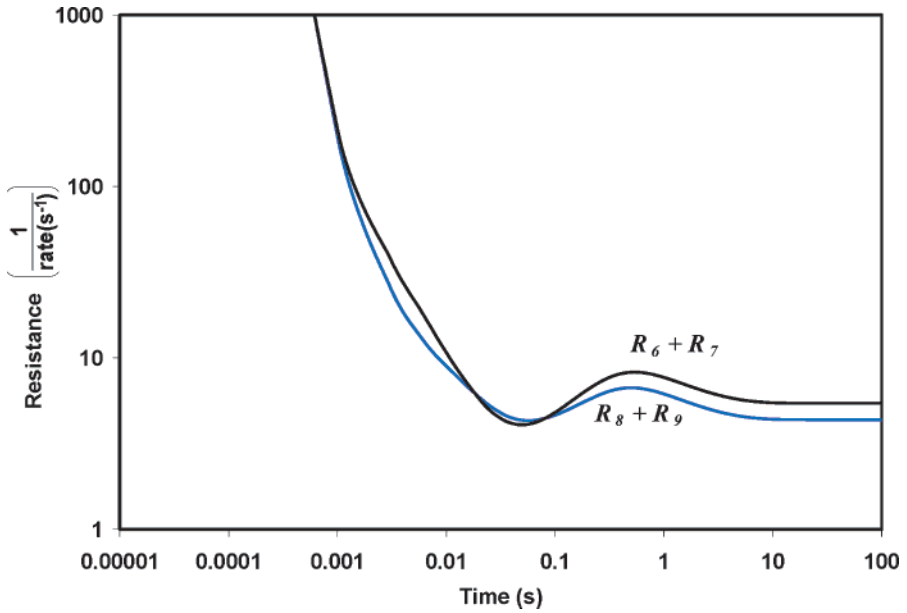

Figure 8. $R_6 + R_7$ vs $R_8 + R_9$, as a function of time for the DHFR reaction in a batch reactor.

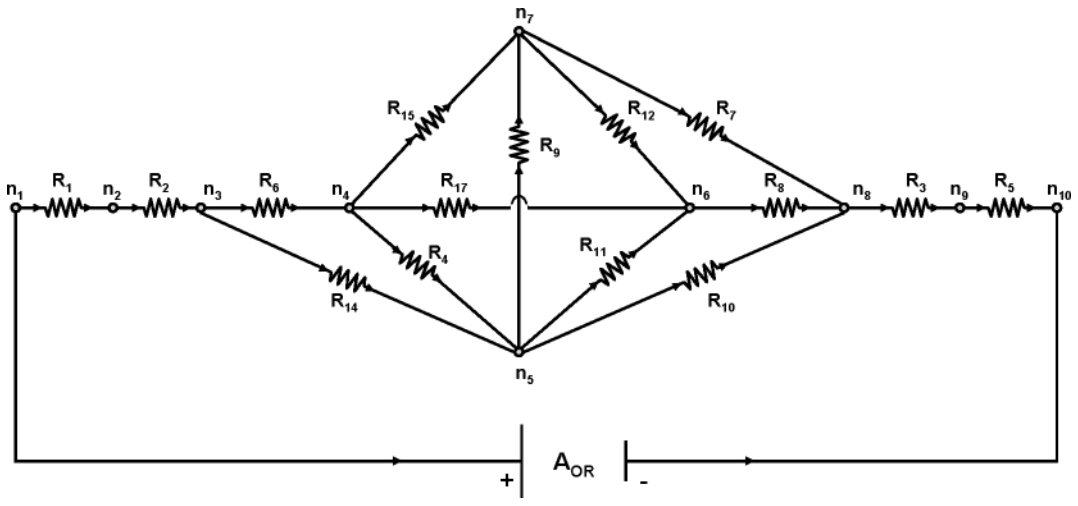

Figure 9. RR network for the water gas-shift (WGS) reaction.

TABLE 3: A Microkinetic Model for the Water Gas-Shift (WGS) Reaction on Copper[a]

step	$\vec{E}_j$	$\vec{A}_j$	elementary reaction step	$\overleftarrow{E}_j$	$\overleftarrow{A}_j$
s_1	0	10^6	$CO + S \leftrightarrows COS$	12.0	10^{14}
s_2	0	10^6	$H_2O + S \leftrightarrows H_2OS$	13.6	10^{14}
s_3	5.3	4×10^{12}	$CO_2S \leftrightarrows CO_2 + S$	0	10^6
s_4	15.3	10^{13}	$HS + HS \leftrightarrows H_2S + S$	12.8	10^{13}
s_5	5.5	6×10^{12}	$H_2S \leftrightarrows H_2 + S$	0	10^6
s_6	25.4	10^{13}	$H_2OS + S \leftrightarrows OHS + HS$	1.6	10^{13}
s_7	10.7	10^{13}	$COS + OS \leftrightarrows CO_2S + S$	28.0	10^{13}
s_8	0	10^{13}	$COS + OHS \leftrightarrows HCOOS + S$	20.4	10^{13}
s_9	15.5	10^{13}	$OHS + S \leftrightarrows OS + HS$	20.7	10^{13}
s_{10}	0	10^{13}	$COS + OHS \leftrightarrows CO_2S + HS$	22.5	10^{13}
s_{11}	1.4	10^{13}	$HCOOS + S \leftrightarrows CO_2S + HS$	3.5	10^{13}
s_{12}	4.0	10^{13}	$HCOOS + OS \leftrightarrows CO_2S + OHS$	0.9	10^{13}
s_{13}	29.0	10^{13}	$H_2OS + OS \leftrightarrows 2OHS$	0	10^{13}
s_{14}	26.3	10^{13}	$H_2OS + HS \leftrightarrows OHS + H_2S$	0	10^{13}
s_{15}	1.3	10^{13}	$OHS + HS \leftrightarrows OS + H_2S$	4.0	10^{13}
s_{16}	0.9	10^{13}	$HCOOS + OHS \leftrightarrows CO_2S + H_2OS$	26.8	10^{13}
s_{17}	14.6	10^{13}	$HCOOS + HS \leftrightarrows CO_2S + H_2S$	14.2	10^{13}

[a] From ref 23. Activation energies given in units of kcal/mol ($\theta \rightarrow 0$ limit), estimated according to ref 24; pre-exponential factors have been taken from ref 14. Pre-exponential factors have been adjusted to fit the thermodynamics of the overall reaction. The units of the pre-exponential factors are $Pa^{-1}\ s^{-1}$ for adsorption/desorption reactions and s^{-1} for surface reactions.

The fundamental cut-set matrix obtained from this $\boldsymbol{\sigma}_f$, as described in Part I,[1] is

$\mathbf{X}_f =$

OR	s_1	s_2	s_3	s_4	s_5	s_6	s_7	s_8	s_9	s_{10}	s_{11}	s_{12}	s_{14}	s_{15}	s_{17}
+1	0	0	0	0	0	0	0	0	+1	+1	+1	0	0	+1	+1
0	+1	0	0	0	0	0	0	0	−1	−1	−1	0	0	−1	−1
0	0	+1	0	0	0	0	0	0	−1	−1	−1	0	0	−1	−1
0	0	0	+1	0	0	0	0	0	−1	−1	−1	0	0	−1	−1
0	0	0	0	+1	0	0	0	0	−1	−1	−1	0	+1	0	0
0	0	0	0	0	+1	0	0	0	−1	−1	−1	0	0	−1	−1
0	0	0	0	0	0	+1	0	0	−1	−1	−1	0	+1	−1	−1
0	0	0	0	0	0	0	+1	0	−1	0	0	+1	0	−1	0
0	0	0	0	0	0	0	0	+1	0	0	−1	−1	0	0	−1

The incidence matrix **M** may be alternately obtained from this by elementary row operations, followed by the addition of a row.

The equations of Kirchhoff's laws are easily obtained from the aforementioned RR cycle matrix, as in the previous example. KCL has two data sets. One is for $\boldsymbol{r}^{(t)} = \boldsymbol{\sigma}_t^T \boldsymbol{J}$:

$$r_{OR} = J_I + J_{II} + J_{III} + J_{VI} + J_{VII}$$
$$r_1 = J_I + J_{II} + J_{III} + J_{VI} + J_{VII}$$
$$r_2 = J_I + J_{II} + J_{III} + J_{VI} + J_{VII}$$
$$r_3 = J_I + J_{II} + J_{III} + J_{VI} + J_{VII}$$
$$r_4 = J_I + J_{II} + J_{III} - J_V$$
$$r_5 = J_I + J_{II} + J_{III} + J_{VI} + J_{VII}$$
$$r_6 = J_I + J_{II} + J_{III} - J_V + J_{VI} + J_{VII}$$
$$r_7 = J_I - J_{IV} + J_{VI}$$
$$r_8 = J_{III} + J_{IV} + J_{VII}$$

and the other data set is that for $\boldsymbol{r}^{(l)} = \boldsymbol{J}$:

$$r_9 = J_I$$
$$r_{10} = J_{II}$$
$$r_{11} = J_{III}$$
$$r_{12} = J_{IV}$$
$$r_{14} = J_V$$
$$r_{15} = J_{VI}$$
$$r_{17} = J_{VII}$$

For KVL,

$$A_{OR} = A_1 + A_2 + A_3 + A_4 + A_5 + A_6 + A_7 + A_9$$
$$A_{OR} = A_1 + A_2 + A_3 + A_4 + A_5 + A_6 + A_{10}$$
$$A_{OR} = A_1 + A_2 + A_3 + A_4 + A_5 + A_6 + A_8 + A_{11}$$
$$0 = A_7 + A_8 + A_{12}$$
$$0 = A_4 + A_6 + A_{14}$$
$$A_{OR} = A_1 + A_2 + A_3 + A_5 + A_6 + A_7 + A_{15}$$
$$A_{OR} = A_1 + A_2 + A_3 + A_5 + A_6 + A_8 + A_{17}$$

Again, KCL provides relationships of elementary reaction step rates and KVL provides expressions for the overall reaction A_{OR} along different reaction routes, as well as illustrating that the net affinity of an empty RR is zero.

3.3. Simplification and Reduction of the RR Graph. When the RR graph is available, the rate of the OR may be evaluated as the ratio of the affinity of the OR and the overall resistance of the equivalent electrical circuit. Because of the complexity of the RR graph, an explicit expression for this is cumbersome and is not given here. Instead, we will first try to simplify and reduce the RR graph by assessing the relative importance of links in parallel pathways between two nodes. Thus, a substantial simplification of the RR graph may be achieved by evaluating and comparing the resistances of the two parallel branches between nodes n_3 and n_5, i.e., the two parallel paths that produce OHS. The first branch involves only one resistance, R_{14}. The second branch involves a sequence of two series resistors—R_4 and R_6—so that its overall resistance is $R_4 + R_6$. An example of numerical simulations of these two resistances, as a function of temperature, is presented in Figure 10. R_{14} is observed to be several orders of magnitude higher than $R_4 + R_6$ at all temperatures. Hence, there is ample justification to neglect s_{14}, which results in the somewhat simplified network shown later in Figure 13b.

The next step in the reduction process is to consider the two parallel branches between nodes n_5 and n_6, that is, R_{11} and $R_9 + R_{12}$. From numerical simulations, it may be concluded (Figure 11) that path s_{11} has a much-lower resistance than path $s_9 + s_{12}$ and, consequently, the latter may be disregarded (see Figure 13c later in this work).

Finally, we compare the resistances of the two remaining parallel branches between nodes n_4, and n_6. One of these two parallel branches involves only one resistance, R_{17}. The other involves resistances R_4 and R_{11} connected in series, with an overall resistance equal to $R_4 + R_{11}$. Based on numerical results (Figure 12), we conclude that the resistance R_{17} is much higher than $R_4 + R_{11}$ and, hence, the consumption of HCOOS via s_{11} is much faster, compared to the consumption of HCOOS via

TABLE 4: Stoichiometrically Distinct RRs for the WGS Reaction on Copper

reaction route	expression
	Full RRs
RR_1	$OR = s_1 + s_2 + s_3 + s_4 + s_5 + s_6 + s_7 + s_9$
RR_2	$OR = s_1 + s_2 + s_3 + s_4 + s_5 + s_6 + s_{10}$
RR_3	$OR = s_1 + s_2 + s_3 + s_4 + s_5 + s_6 + s_8 + s_{11}$
RR_4	$OR = s_1 + s_2 + s_3 + s_4 + s_5 + s_6 + s_8 + s_9 + s_{12}$
RR_5	$OR = s_1 + s_2 + s_3 + s_4 + s_5 + s_6 + s_7 + s_{11} - s_{12}$
RR_6	$OR = s_1 + s_2 + s_3 + s_5 + s_6 + s_7 + s_{15}$
RR_7	$OR = s_1 + s_2 + s_3 + s_5 + s_6 + s_8 + s_{12} + s_{15}$
RR_8	$OR = s_1 + s_2 + s_3 + s_5 + s_7 + s_9 + s_{14}$
RR_9	$OR = s_1 + s_2 + s_3 + s_5 + s_{10} + s_{14}$
RR_{10}	$OR = s_1 + s_2 + s_3 + s_5 + s_8 + s_{11} + s_{14}$
RR_{11}	$OR = s_1 + s_2 + s_3 - s_4 + s_5 + s_7 + s_{14} + s_{15}$
RR_{12}	$OR = s_1 + s_2 + s_3 + s_5 + s_7 + s_{11} - s_{12} + s_{14}$
RR_{13}	$OR = s_1 + s_2 + s_3 + s_5 + s_8 + s_9 + s_{12} + s_{14}$
RR_{14}	$OR = s_1 + s_2 + s_3 - s_4 + s_5 + s_8 + s_{12} + s_{14} + s_{15}$
RR_{15}	$OR = s_1 + s_2 + s_3 - s_4 + s_5 + s_7 - s_{12} + s_{14} + s_{17}$
RR_{16}	$OR = s_1 + s_2 + s_3 - s_4 + s_5 + s_8 + s_{14} + s_{17}$
RR_{17}	$OR = s_1 + s_2 + s_3 + s_5 + s_6 + s_8 + s_{17}$
RR_{18}	$OR = s_1 + s_2 + s_3 + s_5 + s_6 + s_{10} - s_{11} + s_{12} + s_{15}$
RR_{19}	$OR = s_1 + s_2 + s_3 + s_5 + s_6 + s_{10} - s_{11} + s_{17}$
RR_{20}	$OR = s_1 + s_2 + s_3 + s_5 + s_6 + s_7 - s_{12} + s_{17}$
RR_{21}	$OR = s_1 + s_2 + s_3 + s_5 + s_6 + s_7 + s_9 - s_{11} + s_{17}$
RR_{22}	$OR = s_1 + s_2 + s_3 + s_5 + s_6 + s_8 - s_9 + s_{11} + s_{15}$
RR_{23}	$OR = s_1 + s_2 + s_3 + s_5 + s_6 - s_9 + s_{10} - s_{12} + s_{17}$
RR_{24}	$OR = s_1 + s_2 + s_3 + s_5 + s_6 - s_9 + s_{10} + s_{15}$
RR_{25}	$OR = s_1 + s_2 + s_3 + s_5 + s_7 + s_{11} + s_{14} + s_{15} - s_{17}$
RR_{26}	$OR = s_1 + s_2 + s_3 + s_5 + s_8 + s_9 + s_{14} - s_{15} + s_{17}$
	Empty RRs
ER_1	$-s_{12} - s_{15} + s_{17} = 0$
ER_2	$-s_4 - s_{11} + s_{12} + s_{15} = 0$
ER_3	$-s_4 - s_{11} + s_{17} = 0$
ER_4	$-s_4 - s_6 + s_{14} = 0$
ER_5	$-s_4 + s_7 - s_{10} - s_{12} + s_{17} = 0$
ER_6	$s_4 - s_7 + s_{10} - s_{15} = 0$
ER_7	$-s_4 + s_7 - s_8 - s_{11} + s_{15} = 0$
ER_8	$-s_4 - s_7 + s_8 - s_9 + s_{17} = 0$
ER_9	$-s_4 + s_8 - s_{10} + s_{12} + s_{15} = 0$
ER_{10}	$-s_4 + s_8 - s_{10} + s_{17} = 0$
ER_{11}	$-s_4 - s_9 - s_{12} + s_{17} = 0$
ER_{12}	$-s_4 - s_9 + s_{15} = 0$
ER_{13}	$-s_6 + s_{11} - s_{12} + s_{14} - s_{15} = 0$
ER_{14}	$-s_6 + s_{11} + s_{14} - s_{17} = 0$
ER_{15}	$-s_6 - s_7 + s_{10} + s_{12} + s_{14} - s_{17} = 0$
ER_{16}	$-s_6 - s_7 + s_{10} + s_{14} - s_{15} = 0$
ER_{17}	$-s_6 - s_7 + s_8 + s_{11} + s_{14} - s_{15} = 0$
ER_{18}	$-s_6 + s_7 - s_8 + s_9 + s_{14} - s_{17} = 0$
ER_{19}	$-s_6 - s_8 + s_{10} - s_{12} + s_{14} - s_{15} = 0$
ER_{20}	$-s_6 - s_8 + s_{10} + s_{14} - s_{17} = 0$
ER_{21}	$-s_6 + s_9 + s_{12} + s_{14} - s_{17} = 0$
ER_{22}	$-s_6 + s_9 + s_{14} - s_{15} = 0$
ER_{23}	$-s_7 + s_{10} - s_{11} + s_{12} = 0$
ER_{24}	$-s_7 + s_{10} - s_{11} - s_{15} + s_{17} = 0$
ER_{25}	$-s_7 + s_8 + s_{12} = 0$
ER_{26}	$-s_7 + s_8 - s_{15} + s_{17} = 0$
ER_{27}	$-s_7 + s_8 - s_9 + s_{11} = 0$
ER_{28}	$-s_7 - s_9 + s_{10} = 0$
ER_{29}	$-s_8 + s_{10} - s_{11} = 0$
ER_{30}	$-s_8 - s_9 + s_{10} - s_{12} = 0$
ER_{31}	$-s_8 - s_9 + s_{10} + s_{15} - s_{17} = 0$
ER_{32}	$-s_9 + s_{11} - s_{12} = 0$
ER_{33}	$-s_9 + s_{11} + s_{15} - s_{17} = 0$

s_{17}. In other words, the path via s_{17} may be neglected (Figure 13d). The aforementioned simplifications that eliminate four links leave us with a reduced RR network that is comprised of 11 elementary reaction steps and only 3 RRs (namely, RR_{II}, RR_{III}, and RR_{VI}; see Figure 17), rather than the original, a substantial reduction.

The RR network may also be used to generate a reaction energy diagram, as described in Part I.[1] Figure 14 demonstrates this utility of the RR graph theory in systematically composing energy diagrams that are based on forward and reverse activation energies as it applies to the simplified RR network of the WGS reaction (see Figure 13d). In this diagram, each plateau not only represents the resulting species from the preceding surface reactions, but also the corresponding node from the RR network, i.e., n_2 in the network is representative of CO and H_2OS and, similarly, and by convention, the first plateau (labeled "node 2" in Figure 14) is also representative of CO and H_2OS. The three remaining parallel RRs are also evident in this figure as well as the ERs.

3.4. Rate of the Overall Reaction via Electrical Analogy. We are now in a position to consider the rate of the overall reaction. First, we write a formal rate equation for the kinetics of the reduced reaction network (Figure 13d), using the electrical circuit analogy. Thus, the overall rate is the ratio of the affinity of the OR and the overall resistance of the reaction network:

$$r_{OR} = \frac{A_{OR}}{R_{OR}} = \frac{A_{OR}}{R_1 + R_2 + R_3 + R_5 + R_6 + \dfrac{1}{\dfrac{1}{R_7 + R_{15}} + \dfrac{1}{R_4 + \dfrac{1}{\dfrac{1}{R_{10}} + \dfrac{1}{R_8 + R_{11}}}}}} \tag{4}$$

An alternate form of this may be written as below. Keeping in mind that the branch resistance ($R_\rho = A_\rho/r_\rho$) and the affinity of the overall reaction A_{OR} may be expressed via the affinities of the elementary reaction steps, according to the KVL equations, i.e.,

$$\begin{aligned} A_{OR} &= A_1 + A_2 + A_3 + A_4 + A_5 + A_6 + A_{10} \\ &= A_1 + A_2 + A_3 + A_4 + A_5 + A_6 + A_8 + A_{11} \\ &= A_1 + A_2 + A_3 + A_5 + A_6 + A_7 + A_{15} \end{aligned}$$

we finally obtain

$$r_{OR} = \frac{A_1 + A_2 + A_3 + A_4 + A_5 + A_6 + A_{10}}{\dfrac{A_1}{r_1} + \dfrac{A_2}{r_2} + \dfrac{A_3}{r_3} + \dfrac{A_4}{r_4} + \dfrac{A_5}{r_5} + \dfrac{A_6}{r_6} + \dfrac{1}{\dfrac{r_7 r_{15}}{r_{15}A_7 + r_7 A_{15}} + \dfrac{1}{\dfrac{A_4}{r_4} + \dfrac{1}{\dfrac{r_{10}}{A_{10}} + \dfrac{r_8 r_{11}}{r_{11}A_8 + r_8 A_{11}}}}}} \tag{5}$$

This rate equation can be further simplified if the smaller of the resistances in series can be neglected. Furthermore, the affinities of the elementary reaction steps in this equation are not actually all independent, by virtue of KVL. Indeed, Figure 13d shows that the reduced reaction network incorporates three ERs; i.e., the affinities of the elementary reaction steps are interrelated via

$$\begin{aligned} A_7 + A_{15} &= A_4 + A_{10} \\ A_8 + A_{11} &= A_{10} \\ A_7 + A_{15} &= A_4 + A_{11} + A_8 \end{aligned}$$

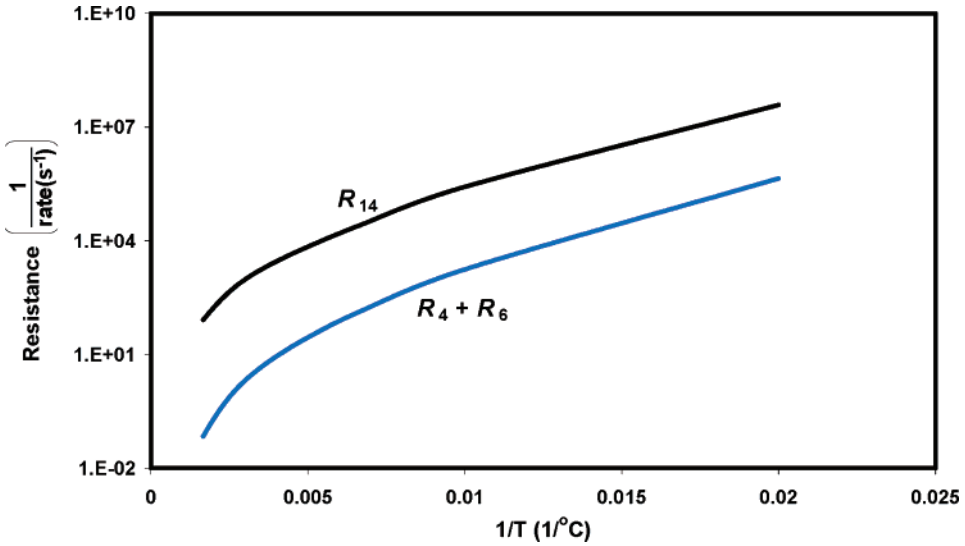

Figure 10. R_{14} vs $R_4 + R_6$, as a function of temperature for the WGS reaction on copper.

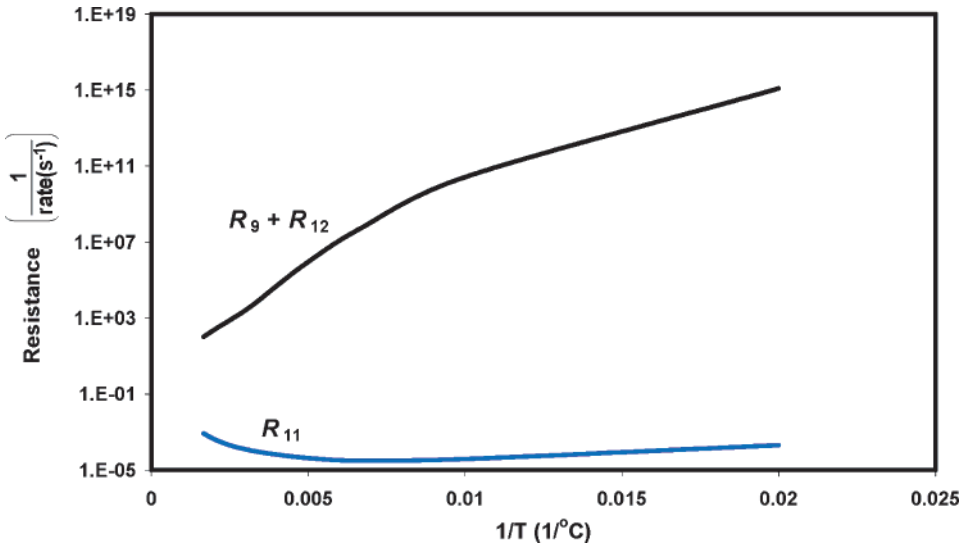

Figure 11. $R_9 + R_{12}$ vs R_{11}, as a function of temperature for the WGS reaction on copper.

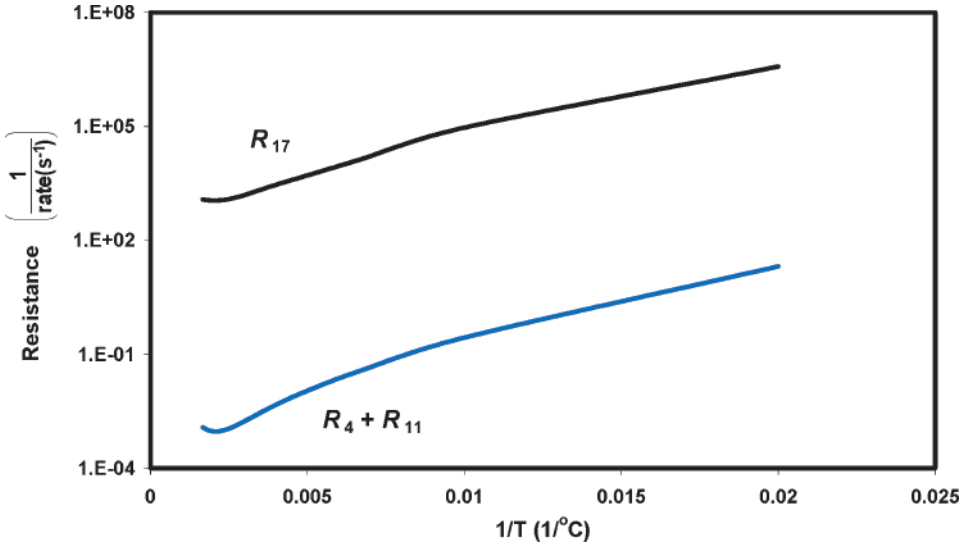

Figure 12. $R_4 + R_{11}$ vs R_{17}, as a function of temperature for the WGS reaction on copper.

Furthermore, not all branch rates are independent. For instance, $r_1 = r_2 = r_3 = r_5 = r_6$, $r_8 = r_{11}$, $r_7 = r_{15}$, etc.

3.5. Explicit Rate Equation. Although the aforementioned formal rate expression is adequate for numerical computation of the rate from numerically calculated resistances, it is more desirable to obtain, if possible, an explicit rate expression in terms of terminal species composition. This is accomplished as follows.

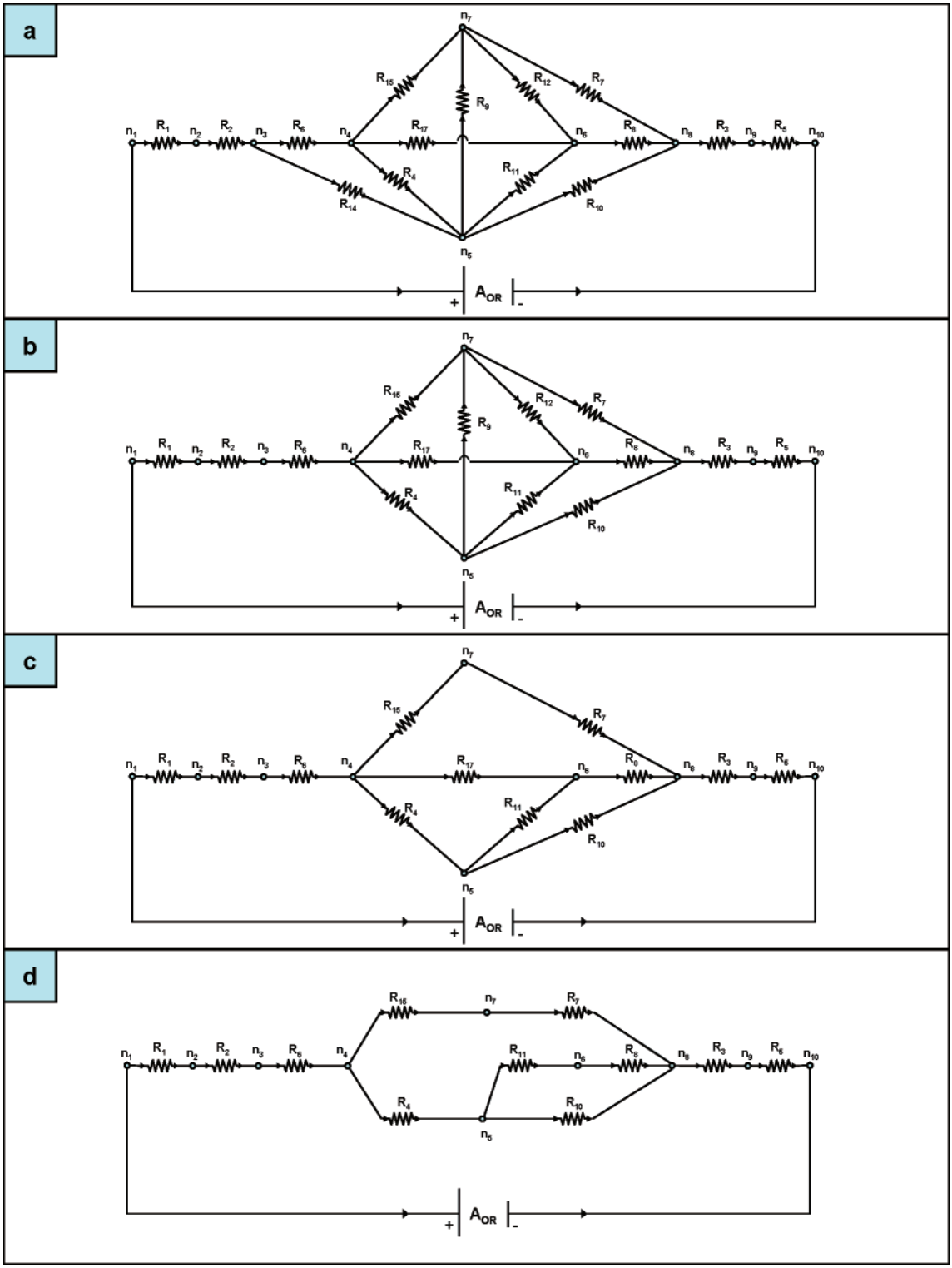

Figure 13. Reduction of the RR network for the WGS reaction on copper.

Because s_9, s_{12}, s_{14}, and s_{17} have been eliminated from the mechanism, there now remain only three linearly independent RRs, namely, RR_{II}, RR_{III}, and RR_{VI}. Thus, KCL for the reduced network provides

$$
\begin{array}{lll}
r_1 = J_{II} + J_{III} + J_{VI} & r_6 = J_{II} + J_{III} + J_{VI} & r_{11} = J_{III} \\
r_2 = J_{II} + J_{III} + J_{VI} & r_7 = J_{VI} & r_{12} = 0 \\
r_3 = J_{II} + J_{III} + J_{VI} & r_8 = J_{III} & r_{14} = 0 \\
r_4 = J_{II} + J_{III} & r_9 = 0 & r_{15} = J_{VI} \\
r_5 = J_{II} + J_{III} + J_{VI} & r_{10} = J_{II} & r_{17} = 0
\end{array}
$$

Furthermore,

$$r_{OR} = J_{II} + J_{III} + J_{VI} = r_8 + r_{10} + r_{15} \qquad (6)$$

which is precisely the same result obtained previously, based on an alternate approach.[22] Concomitantly, this result shows that the rate of the OR expressed via the resistances of the elementary reaction steps (i.e., eqs 4 and 5) is consistent with the conventional rates of the OR.

An explicit overall rate equation may be deduced next by solving the quasi-steady-state (QSS) conditions for the surface

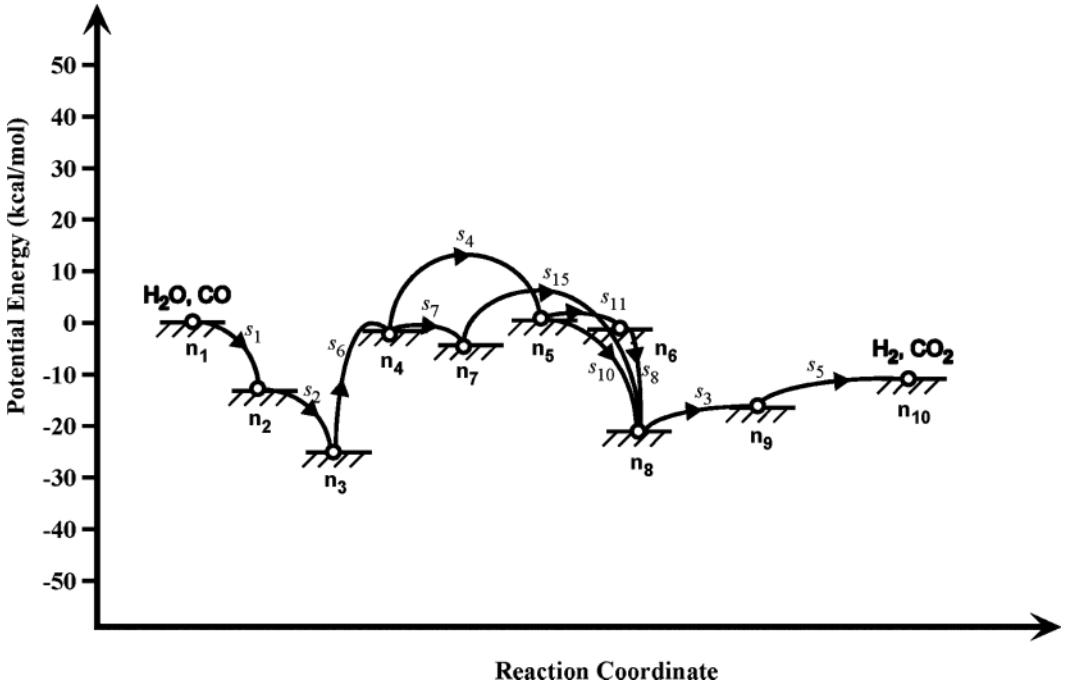

Figure 14. Energy diagram corresponding to the simplified RR graph of the WGS reaction.

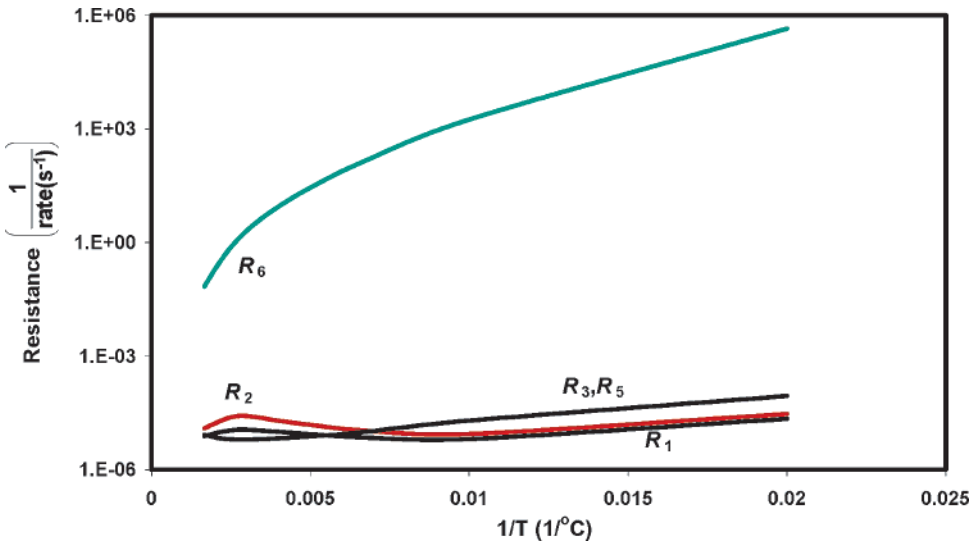

Figure 15. R_1, R_2, R_3, and R_6 versus temperature for the WGS reaction on copper.

intermediates. An analytical solution, however, cannot be obtained, because of the nonlinear character of the resulting equations. To avoid this difficulty, we apply the rate-determining step (RDS) approximation, formulated in terms of resistances. First, we compare the resistances R_1, R_2, R_3, R_5, and R_6 that are in series. Numerical simulations (Figure 15) show that $R_6 \gg R_1$, R_2, R_3, R_5. Thus, in this sequence, s_6 may be considered as an RDS with s_1, s_2, s_3, and s_5 at quasi-equilibrium. This seems to be in agreement qualitatively with Figure 14. In a similar manner, we compare R_4 with $(R_8 + R_{11})R_{10}/(R_8 + R_{10} + R_{11})$ (the overall resistance of the parallel branch following R_4) and conclude that $R_4 \ll (R_8 + R_{11})R_{10}/(R_8 + R_{10} + R_{11})$ (Figure 16). That is, s_4 may also be considered at quasi-equilibrium. Now, the quasi-equilibrium elementary reaction steps may be combined into intermediate reactions, using the formalism of intermediate RRs.[23] The resulting reduced microkinetic model is presented in Table 5. Note that all surface intermediates except OHS and OS may be determined using the quasi-equilibrium approximation. Applying the QSS approximation to OHS and OS, the final simplified overall rate equation is

$$r_{OR} = \frac{\vec{k}_6 K_2 P_{H_2O} \theta_0^2 \left[(\vec{k}_8 + \vec{k}_{10}) K_1 P_{CO} + \vec{k}_{15} \frac{P_{H_2}^{1/2}}{(K_4 K_5)^{1/2}} \frac{\vec{k}_7 K_2 K_5 K_{15} P_{CO}}{\vec{k}_7 K_2 K_5 K_{15} P_{CO} + \vec{k}_{15} P_{H_2}} \right]}{\left[\frac{\vec{k}_6}{K_6} + \vec{k}_{15} \left(\frac{\vec{k}_7 K_2 K_5 K_{15} P_{CO}}{\vec{k}_7 K_2 K_5 K_{15} P_{CO} + \vec{k}_{15} P_{H_2}} \right) \right] \frac{P_{H_2}^{1/2}}{(K_4 K_5)^{1/2}} + (\vec{k}_8 + \vec{k}_{10}) K_1 P_{CO}} \left(1 - \frac{P_{CO_2} P_{H_2}}{K P_{H_2O} P_{CO}} \right) \quad (7)$$

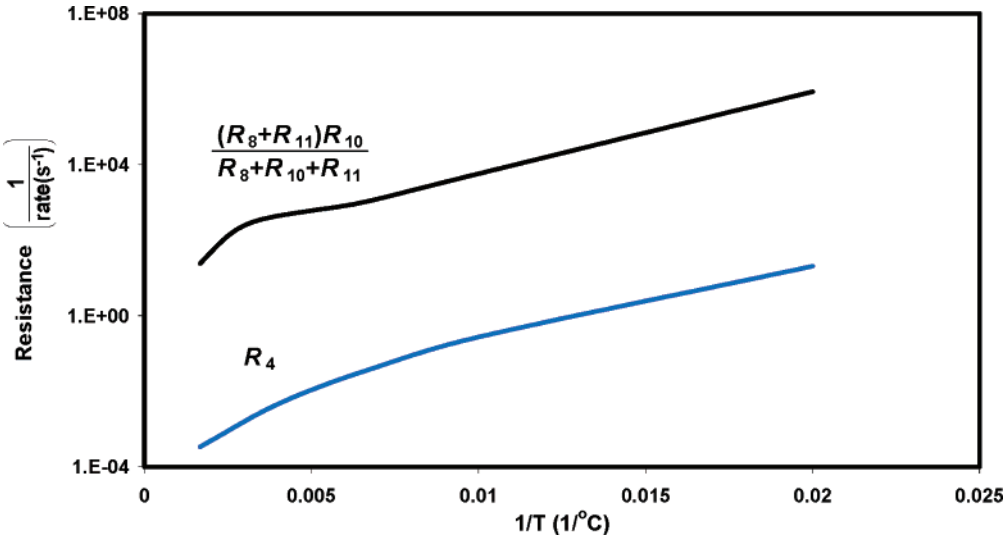

Figure 16. R_4 versus the resistance of the parallel branch involving R_{10}, R_8, and R_{11}, as a function of temperature for the WGS reaction on copper.

TABLE 5: An 11-Elementary Reaction Step Reduced Microkinetic Mechanism for the WGS Reaction on Copper

step	reaction	RR_2	RR_3	RR_6	
s_1	$CO + S \leftrightarrows COS$	1	1	1	EQ
s_2	$H_2O + S \leftrightarrows H_2OS$	1	1	1	EQ
s_6	**$H_2OS + S \leftrightarrows OHS + HS$**	**1**	**1**	**1**	**RDS**
s_7	**$COS + OS \leftrightarrows CO_2S + S$**	**0**	**0**	**1**	**RDS**
s_8	**$COS + OHS \leftrightarrows HCOOS + S$**	**0**	**1**	**0**	**RDS**
s_{10}	**$COS + OHS \leftrightarrows CO_2S + HS$**	**1**	**0**	**0**	**RDS**
s_{11}	**$HCOOS + S \leftrightarrows CO_2S + HS$**	**0**	**1**	**0**	**RDS**
s_{15}	**$OHS + HS \leftrightarrows OS + H_2S$**	**0**	**0**	**1**	**RDS**
s_3	$CO_2S \leftrightarrows CO_2 + S$	1	0	1	EQ
s_5	$H_2S = H_2 + S$	0	0	1	EQ
$^1/_2(s_4 + s_5)$	$HS \leftrightarrows {}^1/_2H_2 + S$	2	2	0	EQ
net	**RR_1: $H_2O + CO \leftrightarrows CO_2 + H_2$**	r_8			
	RR_2: $H_2O + CO \leftrightarrows CO_2 + H_2$	r_{10}			
	RR_3: $H_2O + CO \leftrightarrows CO_2 + H_2$	r_{15}			
	overall rate	$r_8 + r_{10} + r_{15}$			

The error in the conversion of CO provided by this overall rate equation is virtually zero, in comparison with the complete microkinetic model, which points to the robustness of the RR network analysis approach presented here. Furthermore, the expression with predicted rate constants agrees well with experimental data.[23]

4. Discussion and Concluding Remarks

Chemical reactions proceed through a complex network of molecular events, or elementary reaction steps, that involve the reactants, intermediates, and products. After the rate constants of all the elementary reaction steps that comprise a kinetic mechanism are known, the predictions of the kinetic model may be investigated through numerical simulations. However, a complete understanding of the model on the basis of simply numerical computer outputs is difficult to achieve. A large variety of complementary methods, both quantitative and qualitative, have thus been proposed to rationalize the general features of complex kinetic mechanisms. From this arsenal of theoretical methods, two have proved to be of special value in the analysis of kinetic mechanisms. One of these is the reaction routes (RRs) approach, and the other is the graph-theoretical approach. In fact, we show here that these two methods are closely interrelated.[1]

A general limiting feature of the existing graph-theoretical methods,[27] as applied to the analysis of reaction mechanisms,

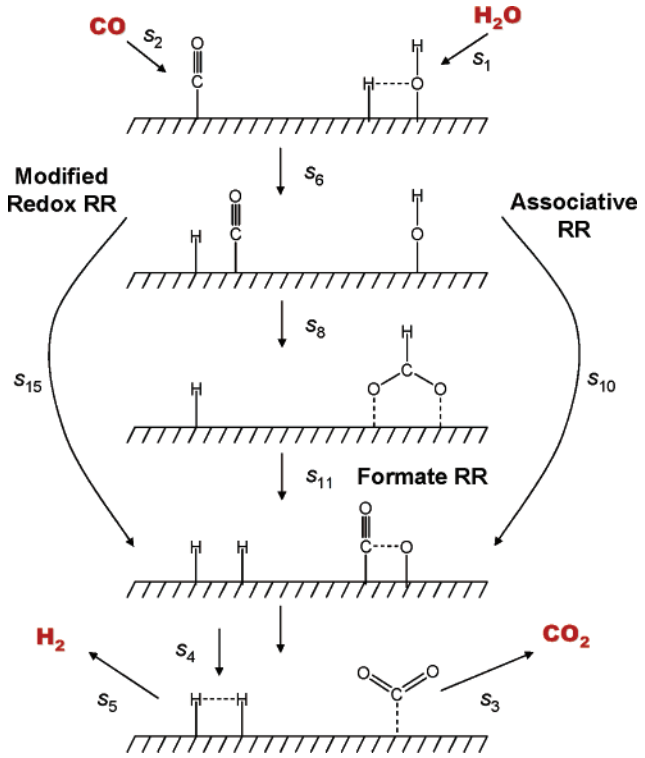

Figure 17. Schematic of the dominant RRs of the WGS reaction on copper.

is that the individual intermediates are represented by the nodes of the graph. Although such a graphical representation is useful in studying many structural aspects of the mechanisms, it is limited to linear mechanisms. As far as we are aware, there have been no previous attempts to overcome this key limitation. In a companion paper (Part I[1]), we showed for the first time that the elementary reaction steps that are comprised of a complex, nonlinear mechanism may be uniquely arranged in a reaction network: the so-called RR graph, in which the nodes simply depict the linking of the elementary reaction steps in a mechanism. The rules that govern the connectivity and directionality of the elementary reaction steps in such a reaction network are derived directly from the quasi-steady-state (QSS) conditions of the surface intermediates. The resulting reaction network incorporates a complete set of direct RRs including

the empty routes (ERs), or cycles, and may be considered as an additional and independent proof of the concept of direct RRs. A subsequent assumption that involves the introduction of the resistance of an elementary reaction step makes the reaction network totally analogous to a linear circuit network. As a result, we are in a position to use the methods of electrical network analysis, including Kirchhoff's Current and Voltage Laws, which represent topological constraints of the network. In particular, the electrical circuit analogy suggests a systematic way of determining the dominant RRs and, hence, a substantial simplification and reduction of the mechanism.

The proposed theoretical methodology[1] has been applied here to study and rationalize two reaction mechanisms and their kinetics. One of these is an enzyme-catalyzed reaction described by a linear kinetic mechanism that is comprised 13 elementary reaction steps. The other is a nonlinear 15-elementary reaction step microkinetic mechanism for the water gas-shift (WGS) reaction on Cu(111). RR graphs for both mechanisms have been constructed such that all of the direct RRs that have been previously generated using the conventional methods are evident. Using the electrical circuit analogy, the reaction networks have been subsequently simplified and reduced. An overall rate equation has been derived based on these simplifications for the WGS reaction that reproduces the complete kinetic mechanism precisely.

In this work, we have discussed only single overall reactions with minimal kinetic mechanisms (unit stoichiometric numbers). For this case, it is possible to construct RR graphs in which each elementary reaction step occurs only once. In subsequent work, we will consider the case of multiple overall reactions. For nonminimal kinetic mechanisms (nonunit stoichiometric numbers), a RR graph that will exactly satisfy the QSS conditions at each node is impossible to construct. Nonetheless, the general theory developed here may be accommodated so as to describe the nonminimal kinetic mechanisms as well. This work will be reported subsequently.

References and Notes

(1) Fishtik, I.; Callaghan, C. A.; Datta, R. *J. Phys. Chem. A* **2004**, *108*, 5671.
(2) Happel, J.; Otarod, M. *J. Phys. Chem. B* **2000**, *104*, 5209.
(3) Fierke, C. A.; Johnson, K. A.; Benkovic, S. J. *Biochemistry* **1987**, *26*, 4085.
(4) Fierke, C. A.; Benkovic, S. J. *Biochemistry* **1989**, *28*, 478.
(5) Andrews, J.; Fierke, C. A.; Birdsall, B.; Ostler, G.; Feeney, J.; Roberts, G. C. K.; Benkovic, S. J. *Biochemistry* **1989**, *28*, 5743.
(6) Thillet, J.; Adams, J. A.; Benkovic, S. J. *Biochemistry* **1990**, *29*, 5195.
(7) Happel, J.; Sellers, P. H. *J. Phys. Chem.* **1992**, *96*, 2593.
(8) Happel, J.; Sellers, P. H. *J. Phys. Chem.* **1995**, *99*, 6595.
(9) Poland, D. J. *Phys. Chem.* **1989**, *93*, 3613.
(10) Chen, T.-S.; Chern, J.-M. *Chem. Eng. Sci.* **2003**, *58*, 1407.
(11) King, E. L.; Altman, C. *J. Phys. Chem.* **1956**, *93*, 6676.
(12) Temkin, M. I. *Adv. Catal.* **1979**, *26*, 173.
(13) Nakamura, J.; Campbell, J. M.; Campbell, C. T. *J. Chem. Soc., Faraday Trans.* **1990**, *86*, 2725.
(14) Satterfield, C. N. *Heterogeneous Catalysis in Industrial Practice*, 2nd ed.; McGraw-Hill: New York, 1991.
(15) Shustorovich, E.; Bell, A. T. *Surf. Sci.* **1991**, *253*, 385.
(16) Ovesen, C. V.; Stoltze, P. J. K.; Nørskov, J. K.; Campbell, C. T. *J. Catal.* **1992**, *134*, 445.
(17) Rhodes, C.; Hutchings, G. J.; Ward, A. M. *Catal. Today* **1995**, *23*, 43.
(18) Vanden-Bussche, K. M.; Froment, G. M. *J. Catal.* **1996**, *161*, 1.
(19) Lund, C. *Ind. Eng. Chem. Res.* **1996**, *35*, 2531.
(20) Ovesen, C. V.; Clausen, B. S.; Hammershøi, B. S.; Steffensen, G.; Askgaard, T.; Chorkendorff, I.; Nørskov, J. K.; Rasmussen, P. B.; Stoltze, P.; Taylor, P. *J. Catal.* **1996**, *158*, 170.
(21) Waugh, K. C. *Catal. Today* **1999**, *53*, 161.
(22) Fishtik, I.; Datta, R. *Surf. Sci.* **2002**, *512*, 229.
(23) Callaghan, C. A.; Fishtik, I.; Datta, R.; Carpenter, M.; Chmielewski, M.; Lugo, A. *Surf. Sci.* **2003**, *541*, 21.
(24) Shustorovich, E.; Sellers, H. *Surf. Sci. Rep.* **1998**, *31*, 1.
(25) Dumesic, J. A.; Rudd, D. F.; Aparicio, L. M.; Rekoske, J. E.; Trevino, A. A. *The Microkinetics of Heterogeneous Catalysis*; American Chemical Society: Washington, DC, 1993.
(26) Fishtik, I.; Callaghan, C. A.; Datta, R. Reaction Network Analysis. The Kinetics and Mechanism of Water-Gas-Shift Reaction on Cu(111). In *Computational Material Science 15*; Leszczynski, J., Ed.; Elsevier: Amsterdam, 2004.
(27) Temkin, O. N.; Zeigarnik, A. V.; Bonchev, D. *Chemical Reaction Networks: A Graph-Theoretical Approach*; CRC Press: New York, 1996.